Dentomaxillofacial Radiology (2018) 47, 20170218

birpublications.org/dmfr

RESEARCH ARTICLE

MR imaging features of mammary analogue secretory carcinoma and acinic cell carcinoma of the salivary gland: a preliminary report

[1]Nobuo Kashiwagi, [2]Shin ichi Nakatsuka, [1]Takamichi Murakami, [3]Eisuke Enoki, [4]Kazuhiro Yamamoto, [5]Katsuyuki Nakanishi, [3]Takaaki Chikugo, [6]Yoshitaka Kurisu, [3]Masatomo Kimura, [1]Tomoko Hyodo, [5]Akio Tsukabe, [7]Takahide Kakigi, [8]Yasuhiko Tomita, [1]Kazunari Ishii, [4]Yoshifumi Narumi, [1]Yukinobu Yagyu and [9]Noriyuki Tomiyama

[1]Department of Radiology, Kindai University Faculty of Medicine, Osaka-Sayama, Japan; [2]Department of Diagnostic Pathology and Cytology, Osaka International Cancer Institute, Osaka, Japan; [3]Department of Pathology, Kindai University Faculty of Medicine, Osaka-Sayama, Japan; [4]Department of Radioligy, Osaka Medical College, Takatsuki, Japan; [5]Department of Diagnostic and Interventional Radiology, Osaka International Cancer Institute, Osaka, Japan; [6]Department of Pathology, Osaka Medical College, Takatsuki, Japan; [7]Department of Radiology, Yamatotakada Municipal Hospital, Yamatotakada, Japan; [8]Department of pathology, International University of Health and Welfare, School of Medicine, Otawara, Japan; [9]Department of Radiology, Osaka University Graduate School of Medicine, Suita, Japan

Objectives: To report MR imaging features of mammary analogue secretory carcinoma (MASC) and acinic cell carcinoma (AciCC) of the salivary gland based on the latest version of the World Health Organization (WHO) 2017 classification of head and neck tumours.
Methods: MR images in 4 patients with MASC and 4 with AciCC were reviewed for margin characteristics, the presence of pathological cervical nodes, the presence of a cystic component and interface between cystic and solid component, signal intensity of the cystic components on T_1 weighted images, and signal intensity of the solid component on T_1 and T_2 weighted images.
Results: All the MASCs and AciCCs had well-defined boundaries, and 1 AciCC had pathological nodes. All 4 MASCs presented as predominantly cystic tumours with papillary projection of the solid component. All 4 AciCCs presented as solid tumours. The signal intensity of the cystic components on T_1 weighted images was entirely hyperintense in 2, and partly hyperintense demonstrating fluid–fluid level in 2. In all the MASCs, the signal intensity of the solid components on T_1 weighted images was intermediate. In the AciCCs, the signal intensity of the solid components on T_1 weighted images was high in 2 tumours and intermediate in 2. The signal intensity of the solid components on T_2 weighted images varied from low to high in both MSACs and AciCCs.
Conclusions: All 4 MASCs had a large cystic component, including areas of high signal intensity on T_1 weighted images. The solid component appeared as a papillary projection into the cystic component. All 4 AciCCs presented as solid tumours, 2 of which showed high signal intensity on T_1 weighted images.
Dentomaxillofacial Radiology (2018) **47**, 20170218. doi: 10.1259/dmfr.20170218

Cite this article as: Kashiwagi N, Nakatsuka Sichi, Murakami T, Enoki E, Yamamoto K, Nakanishi K, et al. MR imaging features of mammary analogue secretory carcinoma and acinic cell carcinoma of the salivary gland: a preliminary report. *Dentomaxillofac Radiol* 2018; **47**: 20170218.

Keywords: MRI; salivary gland; mammary analogue secretory carcinoma; acinic cell carcinoma

Correspondence to: Nobuo Kashiwagi, E-mail: k-nobuo@med.kindai.ac.jp
Received 03 June 2017; revised 18 January 2018; accepted 26 February 2018

Introduction

In the salivary gland section in the most recent edition of the World Health Organization (WHO) classification of head and neck tumours released in 2017, the most significant is represented by mammary analogue secretory carcinoma (MASC), on the basis of morphological similarity and gene mutation to breast secretory carcinomas.[1,2] Most of these tumours had been diagnosed as acinic cell carcinoma (AciCC), due to the morphological resemblance between these two neoplasms.[1–4] This report summarises our early research on the MR imaging findings for MASCs and AciCCs since recognition of MASC as a distinct entity.

Methods and materials

Patients

Tissue blocks were available for 8 of 11 patients with an original diagnosis of AciCC made at any of 3 referring institutions for head and neck tumours over a 12-year period. The tissue blocks for these 8 patients were histologically reviewed for morphology and immunohistochemistry. The tumour morphology was evaluated using sections stained with haematoxylin and eosin based on the published criteria.[2–5] On immunohistochemistry, MASC was diagnosed by co-expression of S-100 and mammaglobin with an absence of DOG1 staining. AciCC was diagnosed by negative or weak expression of S-100 and mammaglobin with positive expression of DOG1 staining.[2–5] Four of the tumours were diagnosed as MASC and 4 as AciCC. The mean age of the 4 patients (2 female, 2 male) with MASC was 31 (range 14–53) years. All tumours were located in the parotid glands. The mean age of the 4 patients (3 female, 1 male) with AciCC was 55 (range 30–68) years. Three of the 4 tumours were in the parotid gland and one was in the oral cavity (buccal mucosa).

Imaging

MR images were obtained using a 1.5 T magnet in 6 patients and a 3.0 T magnet in 2 patients. Axial T_1 and T_2 weighted images were obtained in all patients. Axial short-inversion-time inversion recovery (STIR) images or fat suppressed T_2 weighted were obtained in 4 patients, and diffusion-weighted images were obtained in 3. On coronal sections, STIR or fat suppressed T_2 weighted images were obtained in 7 patients, T_2 weighted images were obtained in 2, and T_1 weighted images with or without a fat suppression technique were obtained in 2. Three patients underwent post-contrast MR images, obtaining both axial and coronal T_1 weighted images with or without a fat suppression technique. The section thickness was 4–5 mm and the pixel size ranged from 0.4 × 0.5 to 0.9 × 0.9 mm.

Data analysis

Two experienced radiologists independently reviewed all MR images with particular attention to the following features: size, margin characteristics, the presence of pathological cervical nodes, internal content, interface between the cystic and solid component, signal intensity of the cystic component on T_1 weighted images, signal intensity of the solid component on T_1 and T_2 weighted images, and apparent diffusion coefficient (ADC) values of the solid component on diffusion-weighted images.

The size was measured as the maximum axial diameter of the lesion. Margin characteristics were classified as well-defined or ill-defined. The lymph node was defined as pathological when it had a minimum axial diameter of 10 mm or central necrosis. Internal contents were classified as solid, predominantly solid, and predominantly cystic, where the cystic component was defined as an area that showed fluid–fluid level or an area of high signal intensity on T_2 weighted images but low signal intensity on diffusion-weighted images or no contrast enhancement. The interface between cystic and solid component was classified as smooth, irregular, and papillary projection, where papillary projection was defined as peripheral papillary-shaped solid component extending to the central cystic component. The signal intensity on T_1 weighted images was defined as follows: low if signal intensity was defined as less than or equal to that of cerebrospinal fluid; intermediate if signal intensity was greater than that of cerebrospinal fluid but less than or equal to that of muscle; and high if signal intensity was greater than that of muscle. The signal intensity on T_2 weighted images was defined as follows: low if signal intensity was defined as less than that of muscle; intermediate if signal intensity was as greater than or equal to that of muscle but less than that of fat; and high if signal intensity was greater than or equal to that of fat. For ADC measurements, regions of interest were manually placed on ADC maps by referring morphological information on T_1 and T_2 weighted images.

Discrepancies between the two readers were resolved by consensus for qualitative evaluations, and measurements of lesion size and ADC were averaged. The intraclass correlation coefficient and kappa κvalue were calculated to evaluate interobserver agreement. The independent *t*-test was used to compare the sizes of MASC and AciCC. A p-value < 0.05 was considered statistically significant. An experienced radiologist and pathologist correlated the MR imaging and pathological findings.

Results

MR imaging features

The clinical information, histological diagnosis, histomorphological growth pattern, and MR imaging features are summarised in Table 1. Representative images are provided in Figures 1–4.The interobserver agreements

Table 1 Summary of histological and MR imaging features

Case number	*Age (years)/ sex*	*Location*	*Histological diagnosis*	*Histomorphological growth pattern*	*Size (mm)*	*Margin characteristics*	*Pathological cervical node*	*Internal content*	*SI of cystic component on T1WI*	*SI of solid component on T1WI*	*SI of solid component on T2WI*	*ADC value of solid component (10^{-3} mm^2 s^{-1})*
1	22/M	Parotid gland	MASC	Papillary-cystic and follicular	34	Well-defined	No	Predominantly cystic	Mixture of intermediate and high (fluid-fluid level)	Intermediate	Mixture of intermediate and high	1.7
2	53/M	Parotid gland	MASC	Papillary-cystic	17	Well-defined	No	Predominantly cystic	High	Intermediate	Intermediate	NA
3	36/F	Parotid gland	MASC	Papillary-cystic and follicular	23	Well-defined	No	Predominantly cystic	Mixture of intermediate and high (fluid-fluid level)	Intermediate	Intermediate	NA
4	14/F	Parotid gland	MASC	Papillary-cystic and follicular	25	Well-defined	No	Predominantly cystic	High	Intermediate	Mixture of intermediate and high	NA
5	30/F	Parotid gland	AciCC	Microcystic and solid	15	Well-defined	No	Solid	NA	High	High	1.1
6	65/M	Parotid gland	AciCC	Microcystic and solid	27	Well-defined	No	Solid	NA	Intermediate	Intermediate	NA
7	68/F	Oral cavity	AciCC	Microcystic and solid	19	Well-defined	No	Solid	NA	High	High	0.37
8	57/F	Parotid gland	AciCC	Solid	64	Well-defined	Yes	Solid	NA	Intermediate	Mixture of low to high	NA

F, female; M, male; NA, not available; SI, signal intensity; T_1WI, T_1 weighted images; T_2WI, T_2 weighted images.

were found to be perfect to substantial, expect for signal intensity of the solid component on T_2 weighted images. The intraclass correlation coefficient was 0.99 for the size and 0.96 for the ADC values. The kappa value was 0.86 for margin characteristic, was 1.00 for the presence of pathological nodes, was 1.00 for internal content, was 0.75 for the interface between the solid and cystic component, was 1.00 for the signal intensity of the cystic components on T_1 weighted images, was 1.00 for the signal intensity of the solid components on T_1 weighted images, and was 0.58 for the signal intensity of solid component on T_2 weighted images. The average maximal cross-sectional diameter of MASCs was 2.5 (range1.7–3.4) cm in MASC and that of AciCC was 3.1 (range1.5–6.4) cm. There was no significant difference in the mean diameter of MASCs and AciCCs. All the MASCs and AciCCs had well-defined margins. One of the AciCCs had pathological lymph nodes. All 4 MASCs presented as predominant cystic tumours, whereas all 4 AciCCs presented as solid tumours. In all 4 MASCs, the interface between the solid and cystic component was classified as papillary projection. The signal intensity of the cystic components on T_1 weighted images showed entirely hyperintense in 2 MASCs and partly hyperintense demonstrating fluid–fluid levels in 2. The signal intensity of the solid components on T_1 weighted images was intermediate in all MASCs. That of AciCC was high in 2 tumours, intermediate in 2 tumours. The signal intensity of the solid component on T_2 weighted images was variable in both MASCs and AciCCs, being high in 2 cases, intermediate in 3, a mixture of intermediate and high in 2, and a mixture of low to high in 1. The ADC values for the solid component were also variable, ranging from 0.3 mm^2 s^{-1} to 18 × 10^{-3} mm^2 s^{-1}.

Correlation between imaging features and histomorphological features

All the MASCs and AciCCs had well-defined margins on MRI imaging, which seemed to reflect that tumours were separated from the normal gland tissue by a fibrous capsule (Figure 1d). All 4 MASCs presented as predominantly cystic tumours with papillary projection. This morphology reflected a histological papillary cystic growth pattern, characterised by marked cystic change with papillary fronds of neoplastic cells (Figure 1d). All 4 AciCCs presented as solid tumours on images, and their histomorphological growth patterns were a mixture of microcystic and solid in 3 cases and solid in one case. On T_1 weighted images, 2 of 4 AciCCs had a hyperintense solid component, which appeared to reflect are as of haemorrhage between the sheets of tumour cells (Figure 3e). The signal intensity of the solid component on T_2 weighted images and the ADC values were variable, which appeared to reflect varying degrees of formation of microcysts in the tumour cells, a desmoplastic stromal reaction, and cellularity.

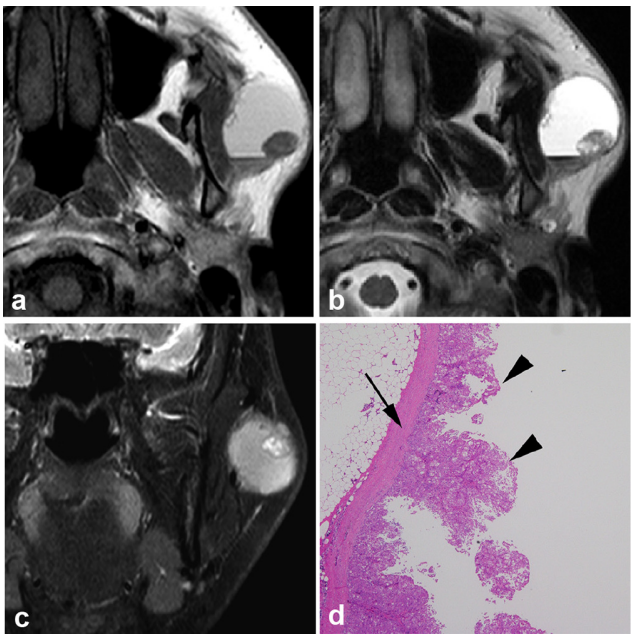

Figure 1 A parotid mammary analogue secretory carcinoma with a papillary-cystic and follicular growth pattern in a 22-year-old male. (a, b) Axial T_1 weighted and T_2 weighted images show a predominantly cystic mass with papillary-shaped solid components extending into the cystic component. The cystic component shows a fluid–fluid level with a hyperintense ventral area. (c) On a coronal STIR image, the solid component shows a mixture of high and intermediate intensity. (d) A photomicrograph of the surgical specimen shows a large cystic component with papillary fronds of neoplastic cells extending into cystic space (arrow heads). The tumour is clearly separated from the normal parotid gland tissue by a fibrous capsule (arrow).

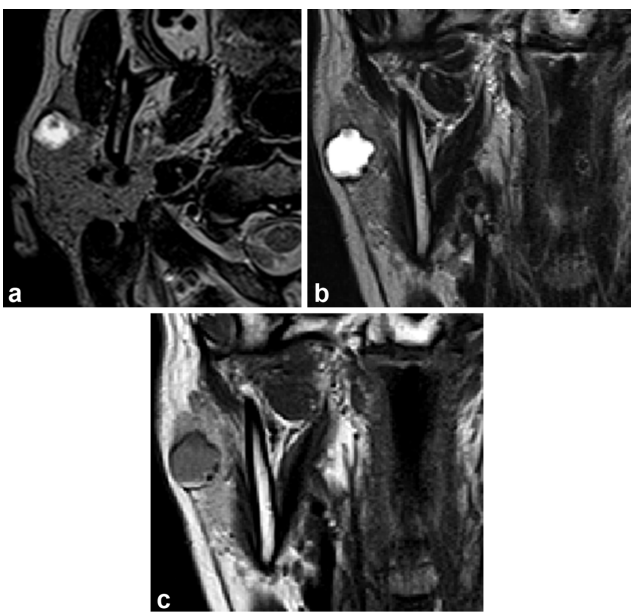

Figure 2 A parotid mammary analogue secretory carcinoma with papillary-cystic growth pattern in a 53-year-old male. (a, b) Axial and coronal T_2 weighted images show a well-defined cystic mass with papillary projections of solid component. (c) On coronal T_1 weighted image, the caudal portion of the cystic component shows high signal intensity.

Discussion

AciCC of the salivary gland is a malignant epithelial neoplasm characterised by the presence of malignant tubular acinar exocrine gland structures, which was described as a distinct entity more than a century ago.[6–8] Since the first description of MASC being extracted from AciCC in 2010,[3] it is widely accepted that MASC is a different entity from AciCC.[1–5,9,10] As for the clinical presentation, both AciCC and MASC share a similar profile with good prognosis and only a few differences have been reported. MASC had equal sex prediction or slight male predominance, in contrast to the female predominance in AciCC, and MASC may have a higher rate of nodal metastases.[2,9,10] Currently, it is unclear whether this separation results in significant clinical impact. However, accumulation of knowledge about the biological behavior of MASC and AciCC may require subtyping of the imaging findings for these two entities.

The present study is the first to report comprehensive MR imaging findings of MASCs and AciCCs and their findings showed a certain tendency. First, all the MASCs and AciCCs had well-defined margins, a low incidence of associated pathological lymph node, and solid components with varying signal intensity on T_2 weighted images. These findings are consistent with low-grade malignancy but overlap with those of benign salivary gland tumours, suggesting the difficulties of differentiating MASCs and AciCCs from benign tumours by MR imaging.

Second, all 4 MASCs were represented as predominantly cystic masses with papillary solid projection, and in contrast, all 4 AciCCs were represented as a solid mass. This difference in imaging between MASCs and AciCCs appeared to well reflect the histomorphological growth pattern. Classically, AciCCs present four major histomorphological growth patterns according to the extent of the cystic portion: solid, microcystic, follicular, and papillary-cystic, the coexistence of different patterns in a single lesion is common.[6–8] The solid pattern is composed of a solid sheet of well-differentiated serous acinar cells with abundant basophilic cytoplasm and variable granularity. The microcystic pattern shows prominent vacuolisation of tumour cells. Enlargement of the microcytic spaces produces a follicular type. Occasional cases are of a papillary-cystic pattern, characterised by a marked cystic change whereby the neoplastic cells are seen to cling to papillary fronds. After MASC was extracted from AciCC, Hsieh et al reported that a common histomorphological feature of MASC is a papillary-cystic pattern without a solid pattern, and that of AciCC is a solid or microcystic pattern.[10] The present study is the first to demonstrate such a tendency of the histomorphological pattern on MR imaging.

In our results, the signal intensity on T_1 weighted images may be noteworthy. In all 4 MASCs, cystic

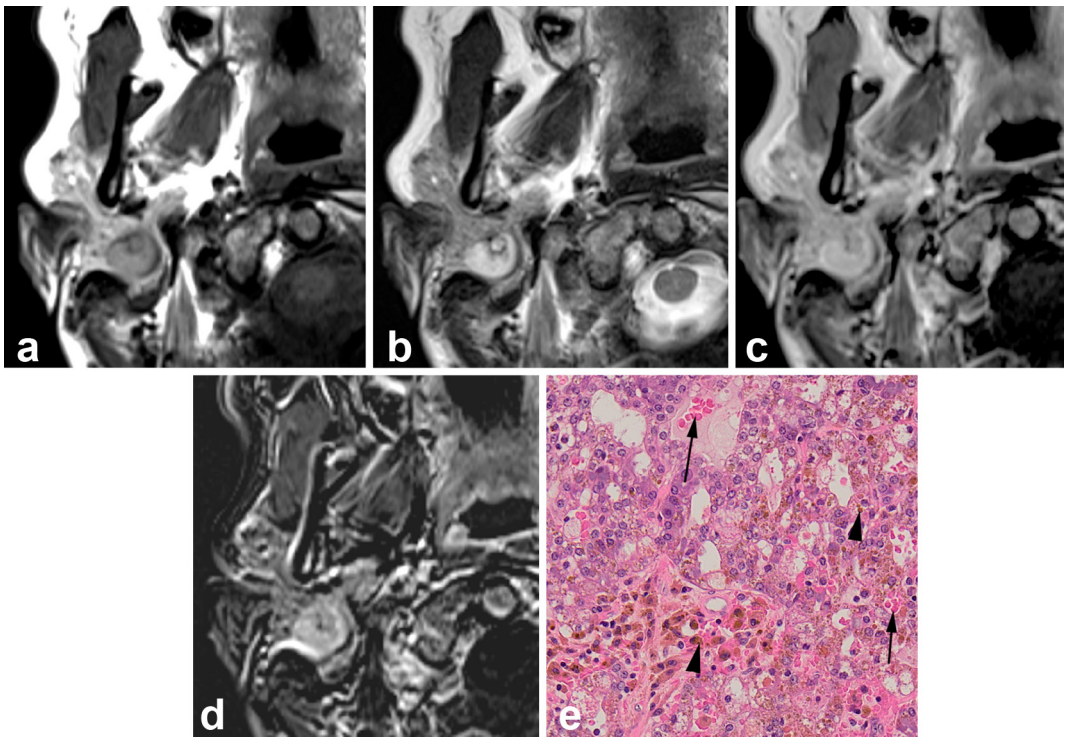

Figure 3 A parotid acinic cell carcinoma with a microcystic and solid growth pattern in a 30-year-old female. (a) Axial T_1 weighted im T_2 weighted image, the mass shows a mixture of high and low intensity. (c, d) Post-contrast T_1 weighted image and subtraction image confirm enhancement of the mass. (e) Photomicrograph of the surgical specimen shows a combination of microcystic spaces and solid neoplastic proliferation. Abundant hemosiderin deposits in the stroma (arrow heads) and erythrocytes in the microcystic spaces (arrows) are seen.

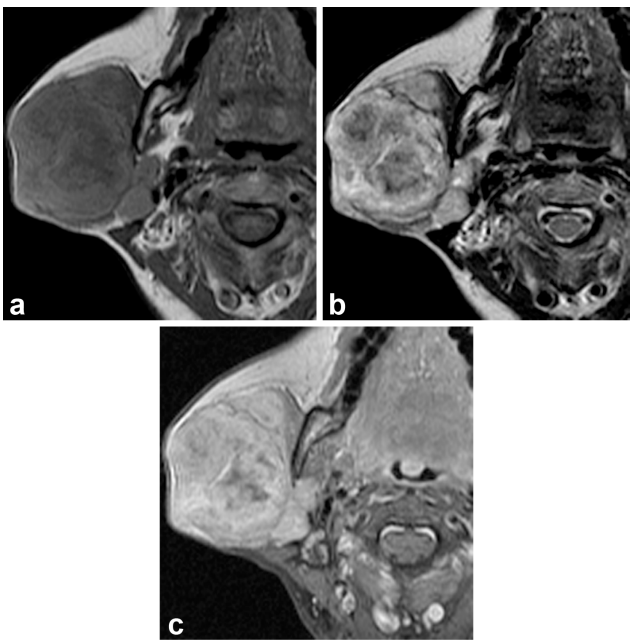

Figure 4 A parotid acinic cell carcinoma with solid growth pattern in a 57-year-old female. (a) Axial T_1 weighted image shows a huge, well-defined mass with intermediate signal and adjacent enlarged lymph nodes. (b) On axial T_2 weighted image, the signal intensity of the mass is a mixture of low to high. (c) Post-contrast T_1 weighted image shows heterogeneous enhancement of the mass.

components showed entirely hyperintense or fluid–fluid level including hyperintense area. These data are not consistent with those in a previous report by Kato et al, who found that a hyperintense cystic component on T_1 weighted images was significantly more common for benign tumours than for malignant tumours.[11] However, their study included only 2 cases of AciCC or MASC with a cystic component. Therefore, when radiologists encounter a salivary gland tumour having a hyperintense cyst on T_1 weighted images, MASC should be included in the differential diagnosis.

Two of the 4 AciCCs in our series presented as hyperintense solid tumours on T_1 weighted images, which may be characteristic. Among the other salivary gland tumours, a hyperintense solid component on T_1 weighted images has only been reported for metastatic malignant melanoma with parotid lymph node involvement.[12] Among the 6 previous reports of MR imaging findings in patients with AciCC, 2 case had hyperintense solid component on T_1 weighted images, but the authors did not speculate on the possible reason for the increased signal.[13–15] With regard to pathological findings, there has been a report of haemorrhages and hemosiderin deposits in the stroma of an AciCC.[10] Our study is the first to report MR imaging features that reflect these pathological findings.

Some published articles have reported the usefulness of the time–intensity curve (TIC) pattern on dynamic

contrast-enhanced MR imaging and calculating ADC in differentiating between malignant tumours, benign non-Warthin tumours and Warthin tumours.[16–20] Most malignant tumours show early enhancement with a low washout ratio with relatively low ADC value (less than 1.4×10^{-3} mm^2 s^{-1}). Benign non-Warthin tumours usually show gradual enhancement with no or minimal washout and relatively high ADC value (greater than 1.4×10^{-3} mm^2 s^{-1}). Warthin tumours usually show early enhancement with a high washout ratio with a low ADC value of around 0.8×10^{-3} mm^2 s^{-1}. In this study, DW images were obtained in only 3 cases, with variable ADC values reflecting variable cellularity. Further studies may indicate whether TIC patterns and ADC values improve the diagnostic accuracy rates for MASCs and AciCCs.

The main differential diagnosis for MASC is a Warthin tumour, because Warthin tumours usually have well-defined margins, and 63% of cases have hyperintense cystic components on T_1 weighted images.[20] With regard to their differentiation, location in the parotid tail suggests a diagnosis of Warthin tumour,[20,21] whereas a younger age (<40 years) and other location in the salivary glands suggest a diagnosis of MASC. In contrast, the differential diagnosis for AciCC includes a wide spectrum of salivary gland tumours because the features of AciCC are non-specific, except for the occasional finding of high signal intensity on T_1 weighted images.

This study has several limitations. First, the small patient population of the study does not allow statistical analysis for characterisation of MR imaging features of MASCs and AciCCs. However, this is the first report on the MR imaging features of MASC and AciCC since recognition of MASC as a distinct entity, so our findings can be considered meaningful. Second, our MASC cases were not subjected to molecular testing for confirmation of ETV6-NTRK3 gene fusion, which had been proposed as the gold standard for diagnosis. However, a recent report mentioned that most cases of MASC can be accurately diagnosed by morphology in conjunction with immunohistochemistry, sufficient for accurate differentiation of MASC from AciCC.[5] Thus, the final histological diagnoses of this study seem to secure accuracy.

In conclusion, to our knowledge, this paper is the first presentation of MR imaging features in MASC and AciCC based on the 2017 WHO classification. MASC tends to present as a predominantly cystic mass with solid papillary projection, whereas AciCC tends to present as a solid tumour. Hyperintensity on T_1 weighted images might be helpful in the diagnosis of AciCC.

Acknowledgements

The authors thank Dr Hiroshi Harada of the Department of Pathology, Fuchu Hospital, for supporting the pathological diagnoses.

References

1. Seethala RR, Stenman G. Update from the 4th edition of the World Health Organization classification of head and neck tumours: tumors of the salivary gland. *Head Neck Pathol* 2017; **11**: 55–67. doi: https://doi.org/10.1007/s12105-017-0795-0
2. Skálová A, Gnepp DR, Lewis JS, Hunt JL, Bishop JA, Hellquist H, et al. Newly described entities in salivary gland pathology. *Am J Surg Pathol* 2017; **41**: e33–e47. doi: https://doi.org/10.1097/PAS.0000000000000883
3. Skálová A, Vanecek T, Sima R, Laco J, Weinreb I, Perez-Ordonez B, et al. Mammary analogue secretory carcinoma of salivary glands, containing the ETV6-NTRK3 fusion gene: a hitherto undescribed salivary gland tumor entity. *Am J Surg Pathol* 2010; **34**: 599–608. doi: https://doi.org/10.1097/PAS.0b013e3181d9efcc
4. Stevens TM, Parekh V. Mammary analogue secretory carcinoma. *Arch Pathol Lab Med* 2016; **140**: 997–1001. doi: https://doi.org/10.5858/arpa.2015-0075-RS
5. Shah AA, Wenig BM, LeGallo RD, Mills SE, Stelow EB. Morphology in conjunction with immunohistochemistry is sufficient for the diagnosis of mammary analogue secretory carcinoma. *Head Neck Pathol* 2015; **9**: 85–95. doi: https://doi.org/10.1007/s12105-014-0557-1
6. Lewis JE, Olsen KD, Weiland LH. Acinic cell carcinoma. Clinicopathologic review. *Cancer* 1991; **67**: 172–9. doi: https://doi.org/10.1002/1097-0142(19910101)67:1<172::AID-CNCR2820670129>3.0.CO;2-X
7. Lin WN, Huang HC, Wu CC, Liao CT, Chen IH, Kan CJ, et al. Analysis of acinic cell carcinoma of the parotid gland - 15 years experience. *Acta Otolaryngol* 2010; **130**: 1406–10. doi: https://doi.org/10.3109/00016481003796801
8. Munteanu MC, Mărgăritescu C, Cionca L, Nițulescu NC, Dăguci L, Ciucă EM. Acinic cell carcinoma of the salivary glands: a retrospective clinicopathologic study of 12 cases. *Rom J Morphol Embryol* 2012; **53**: 313–20.
9. Chiosea SI, Griffith C, Assaad A, Seethala RR. The profile of acinic cell carcinoma after recognition of mammary analog secretory carcinoma. *Am J Surg Pathol* 2012; **36**: 343–50. doi: https://doi.org/10.1097/PAS.0b013e318242a5b0
10. Hsieh MS, Chou YH, Yeh SJ, Chang YL. Papillary-cystic pattern is characteristic in mammary analogue secretory carcinomas but is rarely observed in acinic cell carcinomas of the salivary gland. *Virchows Arch* 2015; **467**: 145–53. doi: https://doi.org/10.1007/s00428-015-1786-8
11. Kato H, Kanematsu M, Watanabe H, Mizuta K, Aoki M. Salivary gland tumors of the parotid gland: CT and MR imaging findings with emphasis on intratumoral cystic components. *Neuroradiology* 2014; **56**: 789–95. doi: https://doi.org/10.1007/s00234-014-1386-3
12. Ismail Y, McLean NR, Chippindale AJ. MRI and malignant melanoma of the parotid gland. *Br J Plast Surg* 2001; **54**: 636–7. doi: https://doi.org/10.1054/bjps.2001.3674
13. Suh SI, Seol HY, Kim TK, Lee NJ, Kim JH, Kim KA, et al. Acinic cell carcinoma of the head and neck: radiologic-pathologic correlation. *J Comput Assist Tomogr* 2005; **29**: 121–6.
14. Sakai O, Nakashima N, Takata Y, Furuse M. Acinic cell carcinoma of the parotid gland: CT and MRI. *Neuroradiology* 1996; **38**: 675–9. doi: https://doi.org/10.1007/s002340050332
15. Sato T, Kamata SE, Kawabata K, Nigauri T, Mitani H, Beppu T, et al. Acinic cell carcinoma of the parotid gland in a child. *Pediatr Surg Int* 2005; **21**: 377–80. doi: https://doi.org/10.1007/s00383-005-1398-5

16. Yabuuchi H, Matsuo Y, Kamitani T, Setoguchi T, Okafuji T, Soeda H, et al. Parotid gland tumors: can addition of diffusion-weighted MR imaging to dynamic contrast-enhanced MR imaging improve diagnostic accuracy in characterization? *Radiology* 2008; **249**: 909–16. doi: https://doi.org/10.1148/radiol.2493072045
17. Razek AA. Diffusion-weighted magnetic resonance imaging of head and neck. *J Comput Assist Tomogr* 2010; **34**: 808–15. doi: https://doi.org/10.1097/RCT.0b013e3181f01796
18. Aghaghazvini L, Salahshour F, Yazdani N, Sharifian H, Kooraki S, Pakravan M, et al. Dynamic contrast-enhanced MRI for differentiation of major salivary glands neoplasms, a 3-T MRI study. *Dentomaxillofac Radiol* 2015; **44**: 20140166. doi: https://doi.org/10.1259/dmfr.20140166
19. Habermann CR, Arndt C, Graessner J, Diestel L, Petersen KU, Reitmeier F, et al. Diffusion-weighted echo-planar MR imaging of primary parotid gland tumors: is a prediction of different histologic subtypes possible? *AJNR Am J Neuroradiol* 2009; **30**: 591–6. doi: https://doi.org/10.3174/ajnr.A1412
20. Ikeda M, Motoori K, Hanazawa T, Nagai Y, Yamamoto S, Ueda T, et al. Warthin tumor of the parotid gland: diagnostic value of MR imaging with histopathologic correlation. *AJNR Am J Neuroradiol* 2004; **25**: 1256–62.
21. Patel DK, Morton RP. Demographics of benign parotid tumours: Warthin's tumour versus other benign salivary tumours. *Acta Otolaryngol* 2016; **136**: 83–6. doi: https://doi.org/10.3109/00016489.2015.1081276